Available online at www.sciencedirect.com
SCIENCE DIRECT®
ELSEVIER
International Journal of Impact Engineering 32 (2006) 1584–1594
INTERNATIONAL JOURNAL OF IMPACT ENGINEERING
www.elsevier.com/locate/ijimpeng

The effect of concrete target diameter on projectile deceleration and penetration depth

D.J. Frew[a,*], M.J. Forrestal[a], J.D. Cargile[b]

[a]*Sandia National Laboratories, Albuquerque, NM 87185-0325, USA*
[b]*US Army Engineer Research and Development Center, Waterways Experiment Station, Vicksburg, MS 39180-6199, USA*

Received 6 September 2004; received in revised form 26 January 2005; accepted 30 January 2005
Available online 11 April 2005

Abstract

We conducted sets of experiments with three diameters of concrete targets that had an average compressive strength of 23 MPa (3.3 ksi) and 76.2-mm-diameter, 3.0 caliber-radius-head, 13-kg projectiles. The three target diameters were $D = 1.83$, 1.37, and 0.91, so the ratios of the target diameters to the projectile diameter were $D/d = 24$, 18, and 12. The ogive-nose projectiles were machined from 4340 R_c45 steel and designed to contain a single-channel acceleration data recorder. Thus, we recorded acceleration during launch and deceleration during penetration. An 83-mm-diameter powder gun launched the 13-kg projectiles to striking velocities between 160 and 340 m/s. Measured penetration depths and deceleration-time data were analyzed with a previously published model. We measured negligible changes in penetration depth and only small decreases in deceleration magnitude as the targets' diameters were reduced.

Keywords: Penetration; Concrete target diameter; Deceleration-time measurements

1. Introduction

Our penetration technology program attempts to provide a fundamental understanding of the penetration process for concrete and geological targets. Early studies for concrete [1–3] and rock

*Corresponding author. Tel.: +1 505 844 7371; fax: +1 505 845 9319.
E-mail address: djfrew@sandia.gov (D.J. Frew).

0734-743X/$ - see front matter © 2005 Elsevier Ltd. All rights reserved.
doi:10.1016/j.ijimpeng.2005.01.012

targets [4,5] used solid, ogive-nose projectiles with diameters between 7 and 30 mm and masses between 0.02 and 1.6 kg. In addition, the target diameter to projectile diameter ratios D/d were between 25 and 30. These studies provided penetration depth versus striking velocity data and information for some empirical penetration models.

More recently, we presented deceleration versus time measurements [6] for ogive-nose, 76.2-mm-diameter, 13-kg projectiles and concrete targets with average compressive strengths of 23 and 39 MPa. These larger diameter projectiles were machined from 4340 R_c 45 steel and designed to contain a single-channel acceleration data recorder [7,8]. Thus, we measured acceleration during launch and deceleration during penetration. For all these studies [1–6], the projectiles lost small amounts of mass through abrasions and experienced relatively small deformations. Therefore, rigid-body deceleration data presented in [6] provides a measure for net force on the projectile nose during the penetration event. The target diameter for that study [6] was 1.83 m and the target diameter to projectile diameter ratio was $D/d = 24$. Thus, the largest target diameter for our early studies with solid rod projectiles [1–3] was 0.91 m; whereas, the target diameter for the projectiles with structurally mounted acceleration data recorders was 1.83 m. For a reasonably complete discussion of the other concrete penetration studies, the readers are referred to the recent paper by Li et al. [9].

The current study was motivated by the ability to perform repeatable concrete penetration experiments at different facilities and at reasonable costs. Since the target volume and mass is proportional to the square of the target diameter, targets with $D/d = 24$ can easily become very expensive or too massive to handle as projectile diameters increase.

In this study, we used the same projectiles, acceleration data recorders [7,8], and 23 MPa strength concrete as that used in our previous study [6]. To examine the effect of concrete diameter on projectile deceleration and penetration depth, we designed a series of experiments with 1.83, 1.37, and 0.91-m-diameter targets. For the 76.2-mm-diameter projectile, $D/d = 24$, 18, and 12. While the post-test, front-face target damage became more severe as D/d decreased, we measured negligible changes in penetration depth and small changes in deceleration magnitudes as D/d decreased. For the authors, these were unexpected results. We anticipated more significant changes in penetration depth and deceleration as D/d decreased by a factor of two.

2. Penetration model

We used our previously published empirical, concrete [6] and rock [4,5] penetration equations to analyze the data. This penetration model was guided by post-test target observations and cavity-expansion analysis [10,11]. The model consists of an entry region with a depth of two projectile diameters followed by a tunnel region. The final penetration depth P for an ogive-nose projectile and a concrete target is given by

$$P = \frac{m}{2\pi a^2 \rho N} \ln\left(1 + \frac{N\rho V_1^2}{R}\right) + 4a, \quad P > 4a, \tag{1a}$$

$$N = \frac{8\Psi - 1}{24\Psi^2}, \quad V_1^2 = \frac{mV_s^2 - 4\pi a^3 R}{m + 4\pi a^3 N\rho} \tag{1b}$$

in which V_1 is the rigid-body projectile velocity when the tunnel region starts at a depth of $4a$, and V_s is the striking velocity. The projectile is described by mass m, shank diameter $d = 2a$, and caliber-radius head ψ. The target is described by density ρ and the target strength parameter R is given by

$$R = \frac{N\rho V_s^2}{\left(1 + \frac{4\pi a^3 N\rho}{m}\right)\exp\left[\frac{2\pi a^2 (P-4a)N\rho}{m}\right] - 1}. \tag{2}$$

As discussed in [4,6], the target resistance parameter is obtained from penetration data. For a set of experiments, we hold all parameters constant and vary striking velocity. From each experiment, we measure striking velocity V_s and penetration depth P, so R can be determined from Eq. (2) for each experiment. We then take the average value of R from the data set and compare predictions from Eq. (1) with the measured values of V_s and P.

This empirical concrete penetration model contains a single parameter called target resistance R, and R is determined from penetration depth versus striking velocity data. Once R is determined, the projectile deceleration versus time can be predicted from the equations given in [1,6]. While this methodology provides a convenient procedure for data analysis, the detailed material response mechanisms for the target are not modeled. Furthermore, Frew et al. [4] and Forrestal et al. [6] have shown that values of R depend on the projectile diameter. Thus, earlier attempts [1–3] to develop concrete penetration equations have been revised to include this observed diameter scale effect [4,6].

3. Experiments

3.1. Concrete targets

In [6], we conducted penetration experiments into 1.83-m-diameter concrete targets with average compressive strengths of $\sigma_{cf} = 23$ and 39 MPa. In this study, we conducted penetration experiments with 1.83, 1.37, and 0.91-m-diameter targets and the same $\sigma_{cf} = 23$ MPa concrete. The 23 MPa concrete used a granite aggregate with a maximum diameter of 9.5 mm. The concrete mix design and physical properties for this concrete are given in Tables 1 and 2 of [6].

Targets were cast in 12 gauge, corrugated steel culverts and 0.60-m-diameter, 0.46-m-long steel drums for material properties tests. Unconfined compression strengths were obtained from 50.8-mm-diameter, 114-mm-long samples cored from the material in the steel drums. We tested 15 samples and obtained an average strength of $\sigma_{cf} = 23$ MPa. Samples for compressive strength tests and targets were allowed to cure for at least 140 days. Strength and penetration tests occurred between 140 and 460 days after the concrete targets were poured.

In addition to the information presented in this study, Warren et al. [12] conducted quasi-static, triaxial material tests with 50.8-mm-diameter, 114-mm-long samples and developed concrete constitutive equations. They developed a continuous surface, porous material, constitutive model-fit to hydrostatic compression, triaxial compression, and uniaxial strain data.

Table 1
Penetration data for concrete targets with nominal compressive strength $\sigma_{cf} = 23$ MPa and 3.0 caliber-radius-head projectiles

Shot and projectile number	Projectile mass (kg)	Target diameter (m)	Target length (m)	Striking velocity (m/s)	Pitch Yaw (degrees)	Penetration depth (m)	R (MPa)
SNL-02-01/1	13.08	1.83	1.37	335	0.9U/0.0	0.94	174
SNL-02-02/2	13.04	1.37	1.52	332	0.1D/0.4R	0.96	167
SNL-02-03/3	13.05	0.91	1.52	337	0.1D/0.7R	1.02	159
SNL-02-08/3	12.89	1.83	1.83	280	0.6D/0.6R	0.73	160
SNL-02-04/4	13.06	1.37	1.22	279	0.2D/0.4R	0.69	173
SNL-02-07/3	12.92	0.91	0.91	201	0.6D/0.6R	0.45	147
SNL-02-06/4	13.00	1.37	0.91	164	0.3U/0.0	0.31	159

For pitch and yaw, D = down, U = up, R = right, L = left.

Table 2
Measured values of striking velocity V_s and penetration depth P given in Table 1. Calculated values of striking velocity V_{sc} and penetration depth P_c from integrations of the declaration versus time data

Shot number	V_s (m/s)	V_{sc} (m/s)	P (m)	P_c (m)
SNL-02-01	335	334	0.94	0.94
SNL-02-02	332	341	0.96	0.98
SNL-02-03	337	344	1.02	1.01
SNL-02-08	280	288	0.73	0.75
SNL-02-04	279	287	0.69	0.70
SNL-02-07	201	N/A	0.45	N/A
SNL-02-06	164	170	0.31	0.32

3.2. Projectiles

Four projectiles, dimensioned in Fig. 1, were machined from 4340 R_c 45 steel. These 76.2-mm-diameter projectiles had 3.0 caliber-radius-head nose shapes and a small conical flare starting at 63.5 mm from the tail end. These projectiles had a nominal mass of 13 kg and were designed to contain a single-channel, acceleration data recorder [7,8].

3.3. Penetration experiments

An 83-mm-diameter, smooth-bore powder gun launched the 13-kg projectiles to striking velocities between 160 and 340 m/s. The projectiles were fitted with sabots and obturators that separated from the projectiles prior to impact. Photographs from a high-speed, digital framing camera (Imacon Model 486) showed the launch packages were stripped from the projectiles prior to impact and these digital photographs were also used to measure pitch and yaw angles. A Hall Intervalometer System measured striking velocities.

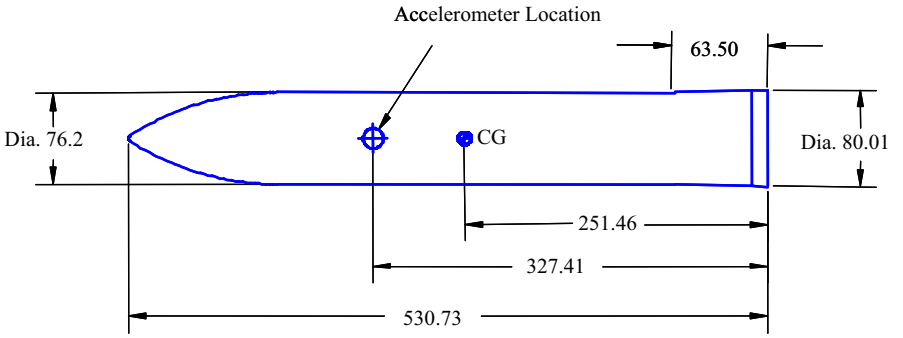

Fig. 1. Geometry and accelerometer location for the 3.0 caliber-radius-head, 13-kg projectile, dimension in millimeter.

Results from the experiments are recorded in Table 1. The first column in Table 1 gives the shot and projectile numbers. For example, in the first line of Table 1, SNL-02-01/1 refers to Sandia National Laboratories, the year (2002), the shot sequence (the first test) and the projectile labeled 1, respectively. Thus, the projectile labeled 1 was launched to a striking velocity of 335 m/s; whereas, the projectile labeled four was first launched to a striking velocity of 279 m/s, and then launched a second time to a striking velocity of 164 m/s. For this test series, abrasion on the projectile surface was negligible, so the shot projectiles were used again without remachining. The last column in Table 1 gives the target resistance parameter calculated from Eq. (2). The average value of R in Table 1 is $R = 163$ MPa, which is in excellent agreement with the average value of $R = 165$ MPa in [6].

In Fig. 2, we show post-test photographs of the 1.83, 1.37, and 0.91-m-diameter targets for striking velocities of 337, 332, and 335 m/s, respectively. These photographs show a dramatic increase in target damage for nearly the same striking velocity as the target diameter decreases. We note that the steel culverts remained intact after the tests.

3.4. Penetration depth and model predictions

Fig. 3 shows penetration depth versus striking velocity for the 23 MPa concrete with density $\rho = 2.04\,\mathrm{Mg/m^3}$ and $R = 165$ MPa. This plot includes six data points from [6] and the data in Table 1 for the three target diameters. All data points lie very close to the model prediction from Eq. (1). Thus, as the target to projectile diameter ratio decreases from $D/d = 24$ to 18 and 12, we observe negligible changes in penetration depth versus striking velocity.

3.5. Projectile deceleration-time measurements and model predictions

As in [6], we conducted penetration experiments that had a single-channel acceleration data recorder structurally mounted within the projectiles. Rohwer [7] describes the development and operation of the single-channel acceleration data recorder called MilliPen. The MilliPen recorder uses an Endevco 7270A accelerometer [8,13] and is designed to digitize and record accelerations during launch and deceleration during penetration. After the penetration event, the projectile is recovered from the target and the recorded digital data is retrieved. Since the projectiles lost small

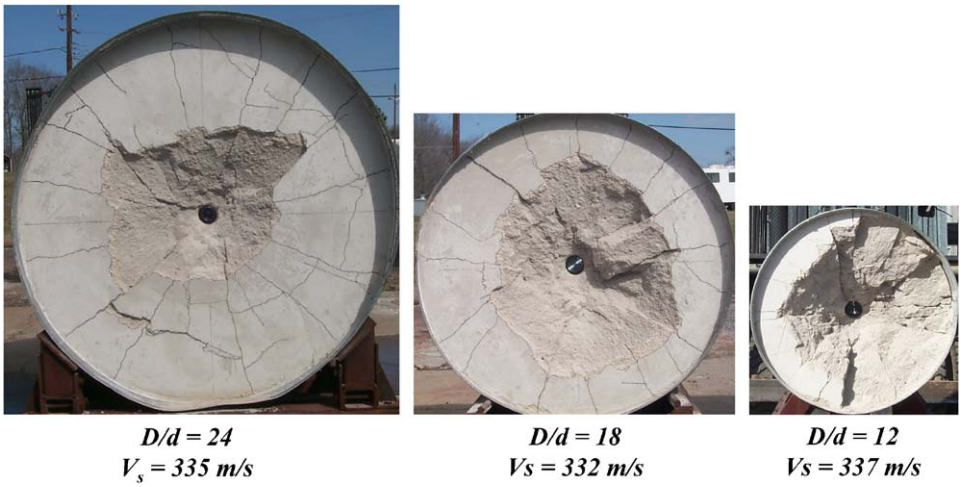

Fig. 2. Post-test photographs of the impact face of the 1.83, 1.37, and 0.91-m diameter targets.

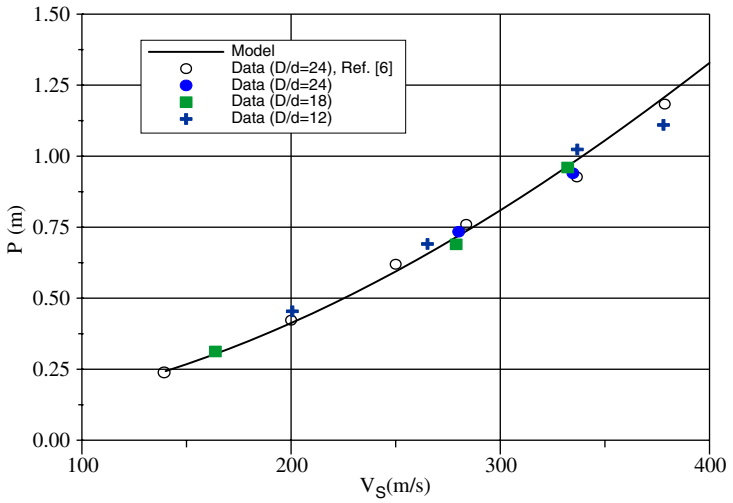

Fig. 3. Penetration depth versus striking velocity for the concrete with average compressive strength $\sigma_{cf} = 23\,\text{MPa}$, density $\rho = 2.04\,\text{Mg/m}^3$, and $R = 165\,\text{MPa}$.

amounts of mass through abrasion and experienced relatively small deformation, rigid-body deceleration data provide a time-resolved measure for net axial force on the projectile during the penetration events.

In Figs. 4–9, we present deceleration versus time measurements for the three nominal striking velocities of 335, 275, and 200 m/s and three target-to-projectile diameters of 24, 18, and 12. Ref. [6] also presents six deceleration versus time measurements for the 13-kg, 3.0 caliber-radius-head projectile into the $\sigma_{cf} = 23\,\text{MPa}$ concrete targets with $D/d = 24$. In [6], we showed that the

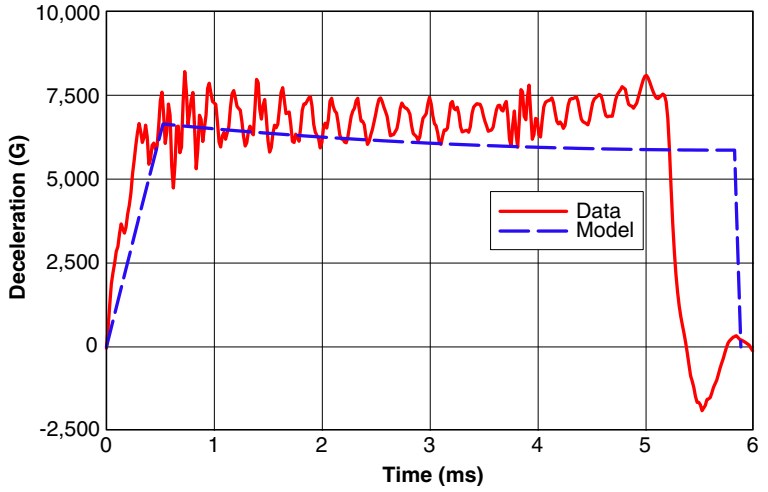

Fig. 4. Deceleration versus time data and model prediction. Shot Number SNL-02-01/1, $D/d = 24$, $V_s = 335\,\mathrm{m/s}$.

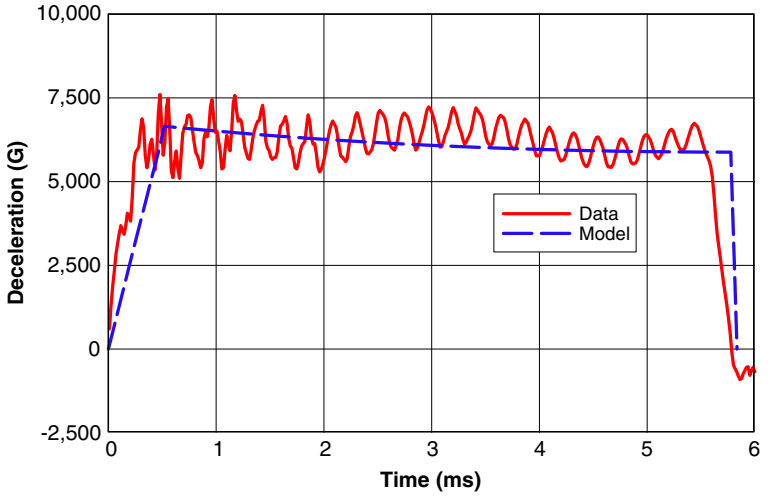

Fig. 5. Deceleration versus time data and model predictions. Shot Number SNL-02-02/2, $D/d = 18$, $V_s = 332\,\mathrm{m/s}$.

penetration model described in this study was in excellent agreement with the deceleration data presented in [6]. Thus, we compare the data in this study with this model to show the effect of decreasing D/d from 24 to 18 and 12.

Figs. 4–6 present data and model predictions for a nominal striking velocity of 335 m/s. As D/d decreases, small deceleration magnitude differences occur as time increases. Figs. 7 and 8 present data and model predictions for a nominal striking velocity of 275 m/s. Again as D/d decreases, small deceleration magnitude differences occur as time increases. Finally, Fig. 9 presents data and model predictions for $V_s = 164\,\mathrm{m/s}$ and $D/d = 18$.

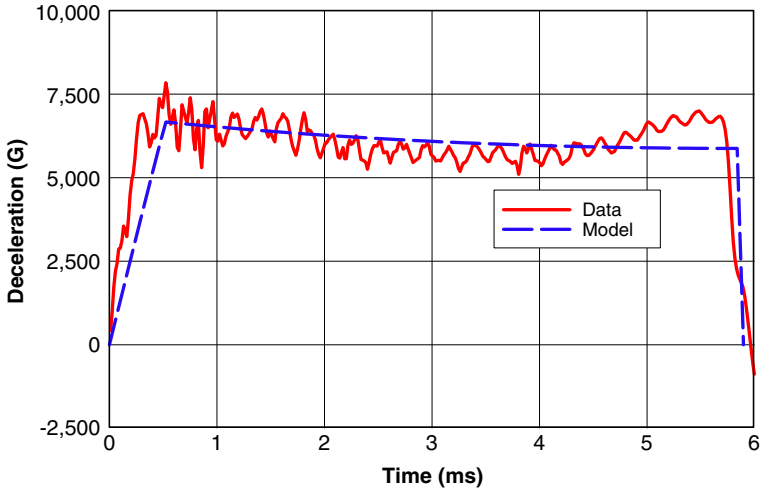

Fig. 6. Deceleration versus time data and model prediction. Shot Number SNL-02-03/3, $D/d = 12$, $V_s = 337\,\mathrm{m/s}$.

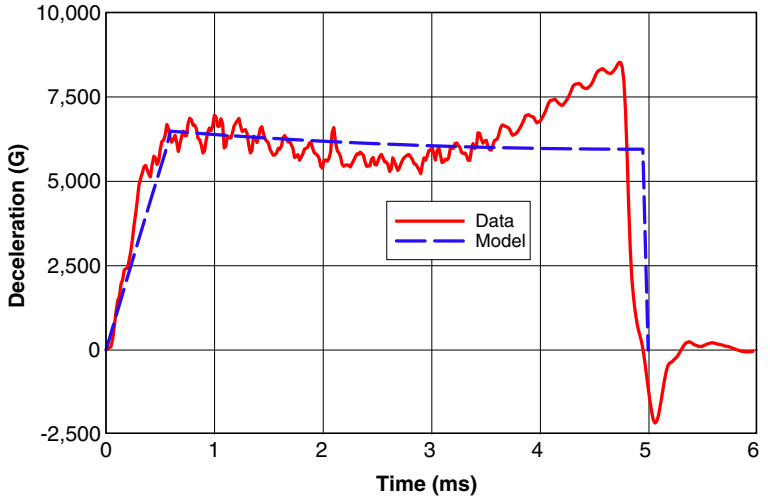

Fig. 7. Deceleration versus time data and model prediction. Shot Number SNL-02-08/3, $D/d = 24$, $V_s = 280\,\mathrm{m/s}$.

To add confidence to the accuracy of the penetration data taken with the MilliPen recorder, we perform integrations of the deceleration-time data to obtain striking velocity and final penetration depth. Thus, we can compare striking velocities measured with the Hall Intervalometer System and an integration of the deceleration-time data, and we can compare final penetration depth with a double integration of the deceleration-time data. Fig. 10 shows single and double integrations of deceleration versus time for penetration experiment SNL-02-02 given in Table 1. These integrations calculate a striking velocity of $V_{sc} = 341\,\mathrm{m/s}$ and penetration depth of $P_c = 0.98\,\mathrm{m}$; whereas, the data in Table 1 give $V_s = 332\,\mathrm{m/s}$ and $P = 0.96\,\mathrm{m}$. These integrations show

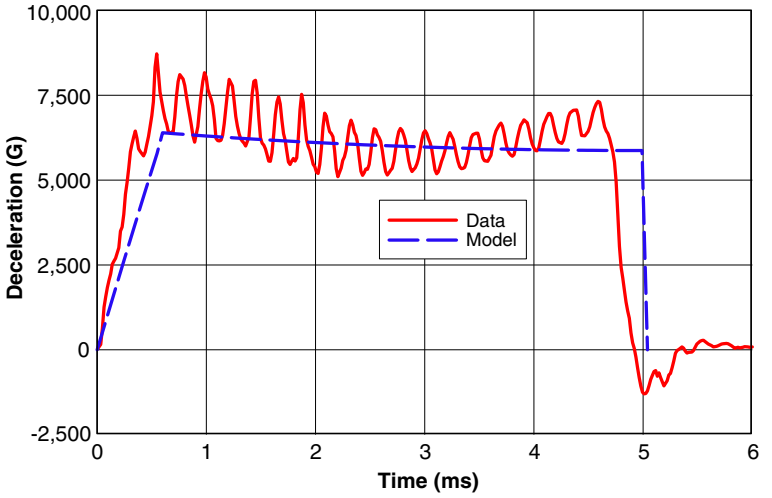

Fig. 8. Deceleration versus time data and model prediction. Shot Number SNL-02-04/4, $D/d = 18$, $V_s = 279\,\mathrm{m/s}$.

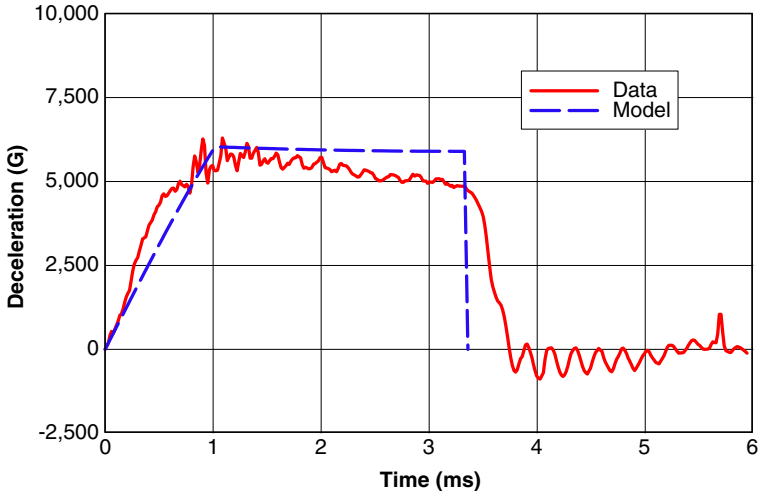

Fig. 9. Deceleration versus time data and model prediction. Shot Number SNL-02-06/4, $D/d = 18$, $V_s = 164\,\mathrm{m/s}$.

good agreement with independent measurements. Table 2 shows comparisons of the values of striking velocity and penetration depth calculated from integrations of the deceleration-time data and those recorded in Table 1. In Table 2, V_s and P refer to the value from Table 1; whereas, V_{sc} and P_c refer to calculated values from the integrations.

3.6. Discussion of results

This study was motivated by the ability to perform repeatable concrete penetration experiments at different facilities and at reasonable costs. Since the target volume and mass is proportional to

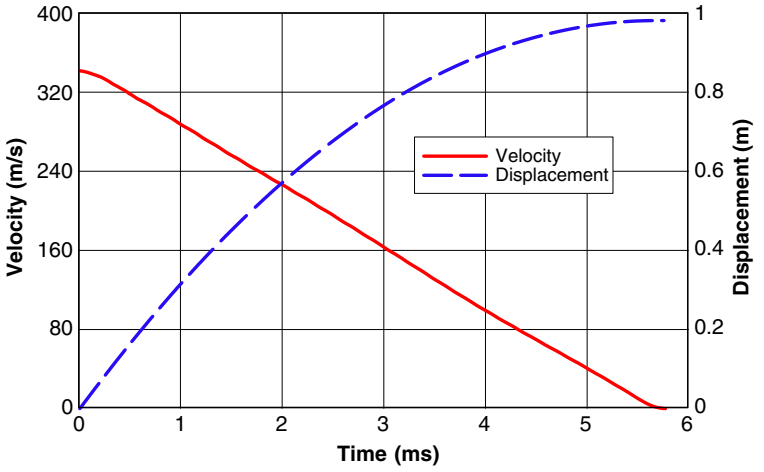

Fig. 10. Projectile velocity and displacement versus time calculated from the deceleration data of Shot Number SNL-02-02.

the square of the target diameter, targets with $D/d = 24$ can easily become very expensive or too massive to handle as projectile diameter increases. While this study showed negligible changes in penetration depth and only small changes in deceleration magnitude as D/d was reduced from 24 to 12, this study cannot be used to draw general conclusions. As with all experimental studies on concrete penetration, the results are dependent on the design parameters. These experiments used the 23 MPa (3.4 ksi) compressive strength concrete described in [6,12], and the targets were cast in 12 gauge, corrugated steel culverts. Perhaps, higher strength concretes or different steel culverts would produce more of an effect than observed in this study. On the other hand, this study offers a procedure to examine the target diameter effect and can help guide the design of other experimental programs for concrete penetration.

4. Summary

We conducted sets of experiments with three diameters of concrete targets that had an average compressive strength of 23 MPa (3.3 ksi) and 76.2-mm-diameter, 3.0 caliber-radius-head, 13-kg projectiles. The three target diameters were $D = 1.83$, 1.37, and 0.91 m. So the ratios of the target diameters to the projectile diameter were $D/d = 24$, 18, and 12. The ogive-nose projectiles were machined from 4340 R_c45 steel and designed to contain a single-channel acceleration data recorder. Thus, we recorded acceleration during launch and deceleration during penetration. An 83-mm-diameter powder gun launched the 13-kg projectiles to striking velocities between 160 and 340 m/s. Measured penetration depths and deceleration-time data were analyzed with a previously published model. While the front face target damage was more severe as D/d decreased, we measured negligible changes in penetration depth and only small decreases in deceleration magnitude as the target diameters were reduced.

Acknowledgements

This work was supported by the Sandia National Laboratories, the Joint DoD/DOE Munitions Technology Development Program, and the US Army Engineer Research and Development Center. Sandia is a multiprogram laboratory operated by Sandia Corporation, a Lockheed Martin Company for the United States Department of Energy's National Nuclear Security Administration under Contract DE-AC04-94AL8500. These experiments were conducted at the Structures and Geotechnical Laboratory, US Army Engineer Research and Development Center, Waterways Experiment Station (ERDC-WES), Vicksburg, MS 39180-6199.

References

[1] Forrestal MJ, Altman BS, Cargile JD, Hanchak SJ. An empirical equation for penetration depth of ogive-nose projectiles into concrete targets. Int J Impact Eng 1994;15:395–405.
[2] Forrestal MJ, Frew DJ, Hanchak SJ, Brar NS. Penetration of grout and concrete targets with ogive-nose steel projectiles. Int J Impact Eng 1996;18:465–76.
[3] Frew DJ, Hanchak SJ, Green ML, Forrestal MJ. Penetration of concrete targets with ogive-nose steel rods. Int J Impact Eng 1998;21:489–97.
[4] Frew DJ, Forrestal MJ, Hanchak SJ. Penetration experiments with limestone targets and ogive-nose steel projectiles. ASME J Appl Mech 2000;67:841–5.
[5] Forrestal MJ, Hanchak SJ. Penetration limit velocity for ogive-nose projectiles and limestone targets. ASME J Appl Mech 2002;69:853–4.
[6] Forrestal MJ, Frew DJ, Hickerson JP, Rohwer TA. Penetration of concrete targets with deceleration-time measurements. Int J Impact Eng 2003;28:479–97.
[7] Rohwer TA. Miniature, single channel, memory-based high-G acceleration recorder (MilliPen). Albuquerque, NM, USA: Sandia National Laboratories; 87185:SAND99-1392C, 1999.
[8] Forrestal MJ, Togami TC, Baker WE, Frew DJ. Performance evaluation of accelerometers used for penetration experiments. Exp Mech 2003;43:90–6.
[9] Li QM, Reid SR, Wen HM, Telford AR. Local impact effects of hard missiles on concrete targets. Int J Impact Eng 2005, to appear.
[10] Forrestal MJ, Luk VK. Penetration into soil targets. Int J Impact Eng 1992;12:427–44.
[11] Forrestal MJ, Okajima K, Luk VK. Penetration of 6061-T651 aluminum targets with rigid long rods. ASME J Appl Mech 1988;55:755–60.
[12] Warren TL, Fossum AF, Frew DJ. Penetration into low strength (23 MPa) concrete: target characterization and simulations. Int J Impact Eng 2004;30:477–503.
[13] Endevco General Catalog, Piezoresistive accelerometer model 7270A, 60 K. 20700 Rancho Viego Road, San Juan Capistrano, CA; 1997.